

Analysis of conveyor belts in winter Mediterranean cyclones

B. Ziv · H. Saaroni · M. Romem · E. Heifetz ·
N. Harnik · A. Baharad

Received: 14 January 2009 / Accepted: 3 May 2009 / Published online: 2 June 2009
© Springer-Verlag 2009

Abstract The relevance of the midlatitude conveyor belt model to Mediterranean cyclones (MCs) is examined using data from two winters. Eight MCs, which exhibit typical midlatitude cyclone structure, were scrutinized and their conveyor belts were examined. The analysis was based on satellite imagery, isentropic wind maps, vertical cross-sections of potential and equivalent potential temperatures, and air back-trajectories. The conveyor belts found in the studied MCs were similar to the common features of midlatitude cyclones, except for three aspects. First, the warm conveyor belt was not associated with massive organized cloudiness in five of the eight cyclones since it consisted of dry air originated from the Saharan desert. Second, the anticyclonic branch of the cold conveyor belt was not found in half of the MCs. Third, the dry air intrusion originated north of the cyclone and extended southward around it, unlike its common midlatitudinal northwest–southeast orientation. This is consistent with the relatively small baroclinic vertical-westward tilt of the cyclones analyzed.

1 Introduction

The conveyor belt model (CBM) describes air motion in the frame of reference of the cyclone track and provides a good framework for understanding the precipitation and cloud fields accompanying midlatitude cyclones during their development (see review articles by Browning 1990 and Carlson 1991). The CBM was developed for and applied to midlatitude cyclones over the US and the main global storm tracks. A somewhat weaker secondary storm track runs along the Mediterranean Basin (MB) and is especially active in the winter season (Hoskins and Hodges 2002). Studies have shown that Mediterranean storms exhibit some characteristics typical of midlatitude storms (e.g., Alpert and Ziv 1989; Alpert et al. 1990, Tsidulko and Alpert 2001) with some differences stemming from the proximity of the Mediterranean to the arid subtropics and an influence of stronger storms over Europe which typically exist alongside the Mediterranean cyclones (MCs).

1.1 The conveyor belt model

The CBM has evolved over many decades of study (starting from Shaw 1903; Kutzbach 1979; Cohen 1993; Wernli 1995; Gall and Shapiro 2000; Schultz 2001 for reviews of the history of the CBM development) before being integrated into the familiar conceptual CBM by Carlson (1980) in an investigation of a winter storm in Central United States in 1977. Carlson's CBM (which was extended further by Browning 1990, 1997, 1999) describes three airstreams affecting the structure of clouds and precipitation—the warm conveyor belt (WCB), the cold conveyor belt (CCB), and the dry air intrusion (DAI). They are identified on isentropic streamline maps of the wind field relative to the cyclone velocity. The horizontal

B. Ziv (✉)
The Open University of Israel,
P.O. Box 808, Ra'anana 43107, Israel
e-mail: baruchz@openu.ac.il

H. Saaroni · M. Romem
Department of Geography and the Human Environment,
Tel Aviv University,
Tel Aviv 69978, Israel

E. Heifetz · N. Harnik · A. Baharad
Department of Geophysics and Planetary Sciences,
Tel Aviv University,
Tel Aviv 69978, Israel

projection of the conveyor belts is shown schematically in Fig. 1.

The WCB is composed of warm air with high moisture content. This belt originates in the subtropics at the lower levels and ascends moving northward, in an anticyclonic curvature, up to ~6,000 m (the midtroposphere; Eckhardt et al. 2004) to the right of the cyclone center. The WCB is about 2,000 km long and 3 km deep. It is represented in the satellite imagery by a thick cloud band curved cyclonically in its southernmost part and anticyclonically at the jet level in its northern part, yielding an “S” shape. Since its associated cloudiness is normally precipitating, the WCB is considered as the main rainfall contributor of the cyclone (Eckhardt et al. 2004). Kurz (1988), Wernli (1995, 1997) Bader et al. (1995), and Browning and Roberts (1996) found that, during the early stages of cyclogenesis, if the upper-level flow is open, i.e., no closed systems exist, the WCB rises to the upper troposphere and turns anticyclonically downstream of the cyclone. Later, during the occlusion stage, if the upper-level flow is characterized by a closed cyclone, some of the WCB may turn cyclonically around the cyclone center (known as the *trowal airstream* of Martin 1999), and in some cases, lead to the formation of a comma-shaped cloud pattern.

The CCB transports cold air that originates from the lower levels, ~1,500 m, northeast of the cyclone center. The air flows westward relative to the cyclone, beneath the WCB, and while passing north of the cyclone center, it splits into two branches, cyclonic and anticyclonic (Carlson 1987; Browning 1990; Carlson 1991). The cyclonic branch encircles the cyclone counterclockwise while descending slightly, whereas the anticyclonic branch turns sharply clockwise, northeastward, and ascends until it merges with the northeastern part of the WCB. Schultz (2001) argued that the anticyclonic branch is very thin. Though the cold air mass in this belt is originally dry, it

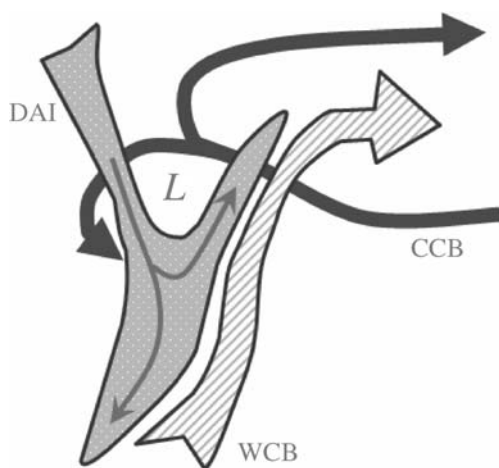


Fig. 1 Schematic structure of the conveyor belts

may become wet due to evaporation from the rain associated with the WCB while it flows below it (Fig. 1). The latent heat release within the upper layer of the CCB tends to increase the potential vorticity (PV) that it advects westward, toward the lower-tropospheric cyclone center. The clouds associated with the cyclonic branch of the CCB are mostly medium and low and produce smaller amounts of rain than in the WCB. Since the precipitation generated within the WCB falls through the CCB, the temperature and humidity of the CCB determines the type and amount of precipitation reaching the surface (ranging from virga, via sleet and freezing rain, and up to an abrupt change from rain to heavy snow; Kain et al. 2000).

The DAI originates from the northwest sector of the cyclone, at the upper troposphere and lower polar stratosphere, and descends on the west side of the upper-level trough, west of the cyclone center (Fig. 1). This air mass is dry and stable with high PV, of ~5 potential vorticity units (PVU) typically. The DAI encircles the cyclone cyclonically through its southwest part, behind the cold front. While descending into the subtropical troposphere, it attains a “hammerhead” shape. The DAI plays a significant role in baroclinic cyclogenesis and in the mesoscale convective destabilization that affects clouds development (Carr and Millard 1985; Young et al. 1987; Durran and Weber 1988; Gurka et al. 1995; Browning and Golding 1995; Browning 1997).

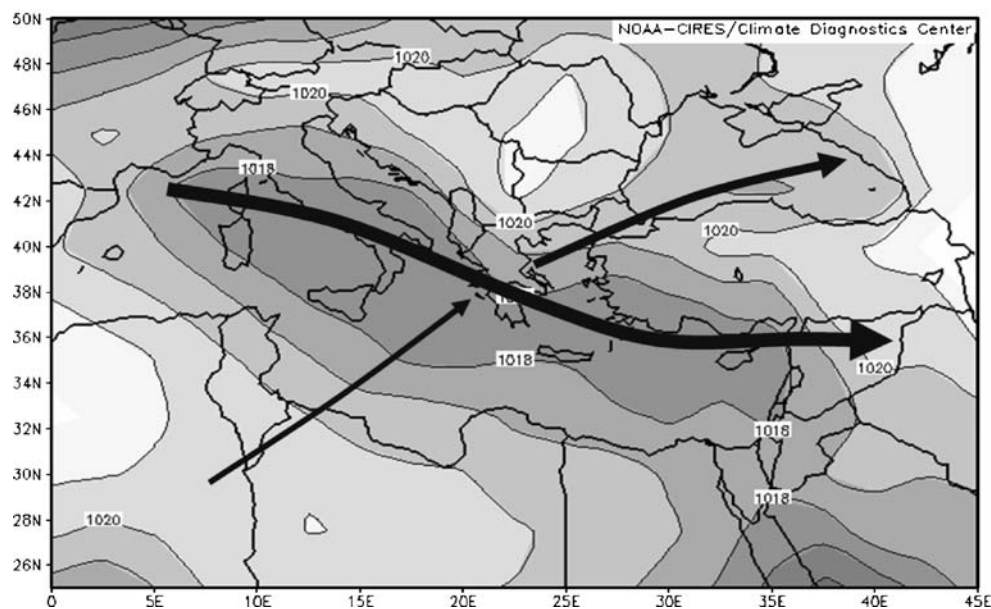
Most of the literature on CBM explored extratropical cyclones in Europe, North America and the Atlantic, or the Pacific Oceans. In this study, we focus on MCs and examine the relevancy of the CBM to their structure and resulting weather conditions.

1.2 Mediterranean cyclones

The MB is highly populated by cyclones, especially in the winter season (HMSO 1962; Reiter 1975; Radinovic 1987; Campins et al. 2000; Romem et al. 2007). The MCs are considered to be of midlatitude frontal type (in spite of being located south of the global midlatitude climatic belt) with a cyclogenetic contribution of orography (Tafferner and Egger 1990; Stein and Alpert 1993). The annual number of MCs varies along the MB, reaching its maximum near the Gulf of Genoa, ~80 (Campins et al. 2000). Their horizontal size differs between mesoscale (Alpert et al. 1999) and synoptic-scale (Campins et al. 2000; Trigo et al. 2002). The MCs tend to propagate eastward along the northern coast of the Mediterranean until reaching the Levant region where they weaken or even dissipate (Kahana et al. 2002). The main MCs’ tracks for January are shown in Fig. 2.

The CBM has been examined for the MCs only partly. Eckhardt et al. (2004), in their climatological study of

Fig. 2 Winter MCs tracks, represented by the long-term mean SLP for January, based on NCEP/NCAR reanalysis data (Kalnay et al. 1996; Kistler et al. 2001). The *thick arrows* represent the main tracks, as inferred from the individual tracks for January 1983–1988 (after Alpert et al. 1990). Their thickness is proportional to the track population



WCBs based on a Lagrangian approach, found a weak signal in the Mediterranean, implying that strong ascent of air masses also occurs in this area of the globe. Other two studies point at the relevance of conveyor belts for this region. One describes a dust plume, “which was transported northward more than 2400 km” and its western boundary coincided with a cold front (Alpert and Ganor 1994). This dust plume reflects, presumably, a WCB which extended from the Sahara northward over the Mediterranean Sea. A second study dealt with the role of high-PV advection in the genesis of a Genoa Low (Tsidulko and Alpert 2001), which resembles the existence of a DAI.

This paper studies the analogy of the MCs to the typical midlatitude cyclones by examining to what extent the CBM holds for the Mediterranean and, correspondingly, whether the main precipitation and cloud features arise due to similar processes. It analyses the 3-D flow structure of MCs, identifies the conveyor belts, and compares their structure with the classical CBM. Section 2 specifies the data and methodology used. Section 3 presents the results for the analyzed MCs and Section 4 summarizes the results and discusses their dynamic and some of their climatological implications.

2 Data and methodology

We examined the MCs during two winters (December–March of 2001/2002 and 2002/2003). The data base is the six hourly National Centers for Environmental Prediction/National Center for Atmospheric Research (NCEP/NCAR) reanalysis (Kalnay et al. 1996; Kistler et al. 2001) with a $2.5 \times 2.5^\circ$ spatial resolution. The eight cyclones selected

were well-developed, with a central vorticity of $>2 \times 10^{-5} \text{ s}^{-1}$, with a diameter of $>1,500 \text{ km}$, and with no additional cyclone in the range of 2,000 km. Each of them existed at least 36 h. The characteristics of the selected cyclones are listed in Table 1. Their typical diameter and speed generally agree with that evaluated by Alpert and Ziv (1989), being $>1,500 \text{ km}$ and 5 m s^{-1} , respectively, and the average value of their central vorticity ($3.5 \times 10^{-5} \text{ s}^{-1}$) is close to those found by Alpert and Neeman (1992) and Trigo et al. (2002).

The identification of the conveyor belts is based on a “semi-Eulerian” approach, i.e., along streamlines of the relative wind field (the wind velocity with respect to the cyclone velocity) on isentropic surfaces, following Browning (1990). The cyclone velocity was determined by tracking its center along 12-h intervals around the pertinent time. Since the conveyor belts were found in various heights throughout the troposphere, the use of the surface cyclone alone did not seem to be proper for tracking it. We, therefore, averaged the flow over the 1,000- to 300-hPa range. In this averaging, closed cyclones were not always found (but open troughs), so we used the relative vorticity maximum to represent the cyclone center.

The isentropic surfaces better approximate the actual air movement than the pressure surfaces do. But, since condensation exists along conveyor belts, with its implied latent heat release, the isentropic surfaces may be poor approximation where condensation takes place, so that air changes its potential temperature (θ). In that case, the air conserves only its equivalent potential temperature (θ_e), implying that it moves along θ_e surfaces. However, the use of θ_e surfaces for analyzing conveyor belts was found impractical because, in several cases, θ_e did not increase

Table 1 General features of the eight studied MCs

Dates of existence	500-hPa system	Diameter (km)	Min SLP (hPa)	Average speed (m s ⁻¹)	Max vorticity at 295°K (10 ⁻⁵ s ⁻¹)
16–18 Jan 2002	Cutoff low	1,800	1,017	5.8	4
10–13 Mar 2002	Cutoff low	1,900	1,005	7.5	5
22–23 Mar 2003	Open trough	2,000	997	9.6	4
6–8 Jan 2003	Open trough	1,700	995	9.6	5
10–12 Jan 2003	Cutoff low	1,900	994	12.6	5
17–20 Jan 2003	Open trough	2,150	1,013	6.6	4
26–28 Jan 2003	Cutoff low	2,200	1,004	6.5	4.5
31 Jan–2 Feb 2003	Open trough	1,600	1,000	8.6	6
Average		1,900	1,003	8.4	4.5

The cyclone diameter was defined with respect to the region of positive relative vorticity at the 295°K isentropic level

with height but remained constant. In order to assess the validity of using isentropic sections, we examined the Lagrangian θ change of individual air parcels traveling along the conveyor belts. The largest changes were found in the WCBs, being $<3^\circ\text{K}$ within 12 h. This suggests that, for our practical needs, isentropic sections are sufficient.

The locations of the WCB and the CCB were determined subjectively along bands of streamlines which coincided with a tongue of warm or cold air, searching for features that meet the “classical” description (e.g., Browning 1990). A “tongue” is represented by a trough or a ridge in the geometry of the isentropic surface along the WCB and the CCB, respectively. The WCBs were searched along the southerly flow separating between the cyclone to the west and the anticyclonic circulation to the east. The CCBs were searched, starting from the cold reservoir north of the cyclone and encircling the cyclone from the west. The choice of the representative isentropic level for each conveyor belt was done by inspecting the isentropes (in 2°K increments) ranging from 298 to 316°K for the WCB and from 284 to 302°K for the CCB. The actual level for each type of conveyor belt differed from one case to another. The conveyor belts found in the isentropic maps were also searched for in the IR METEOSAT satellite imagery, attempting to identify cloud bands that coincide with them. The images used were of 6- to 8-km resolution and could not enable us to differentiate between convective and stratified clouds confidently. For some of the cases, MODIS images of 2-km resolution (http://www.nasa.gov/about/highlights/HP_Privacy.html#links) were available and were used to augment the analysis.

The DAI was identified in the isentropic level that best represents the tropopause, i.e., in which positive PV anomalies exceed 2 PVU. This threshold follows Browning (1990), Wernli (1997), and Wernli and Davies (1997). It was depicted along anomalously high-PV bands connected to the high-PV reservoir to the north, parallel to the

streamlines. In order to further assess the stratospheric source of the DAI, a relative humidity (RH) map was derived. Pattern of low values that coexist with a high-PV anomaly is very suggestive of a stratospheric source.

To better elucidate the thermodynamic characteristics of the air masses within the conveyor belts, we analyzed them also by vertical cross-sections of θ_e , calculated following Bolton (1980). Since θ_e is conserved during condensation, layers that are subjected to moist convection would have zero vertical θ_e gradient, combined with high RH. The difference, $\theta_e - \theta$, is a measure for specific humidity, as it is higher in moist regions. Following the above, θ_e can be considered as an efficient tracer and conveyor belts are expected to appear as slanted layers of relatively constant high or low θ_e (when the air mass transported is moist or dry relative to its surrounding, respectively).

In order to identify the sources of the air masses within the conveyor belts, we derived back-trajectories of air parcels located at significant reference points on the conveyor belts, using the National Oceanic and Atmospheric Administration HYSPLIT4 (Hybrid Single-Particle Lagrangian Integrated Trajectory) Model (1997).

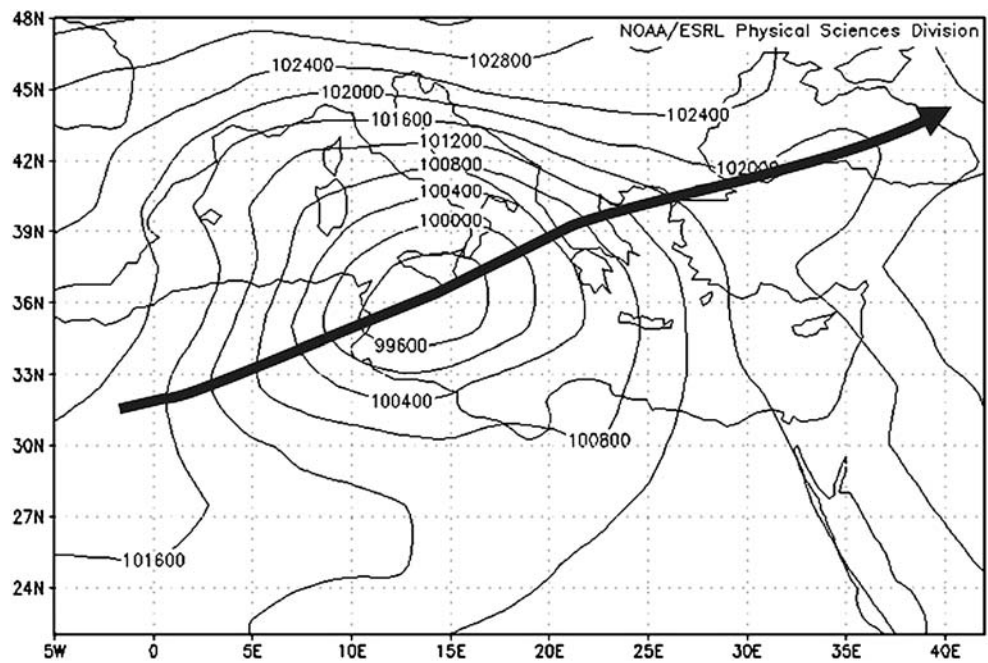
3 Results

The main features of the studied cyclones and the methodology applied are exemplified by a case study presented in the following subsection. The CBM structure in this case is characteristic of the other MC cases examined.

3.1 A case study: 10–12 January 2003

This cyclone was formed on 9 January 2003 18 UTC in Alger, at 30°N , 2°W , and existed for 72 h. The cyclone moved east–northeastward at an average speed of 13 m s^{-1} ,

Fig. 3 SLP for January 11, 2003, 06 UTC and the trajectory of the cyclone



until it reached the eastern part of the Black Sea (44° N, 40° E). Its minimum sea-level pressure (SLP) was 994 hPa and the maximum relative vorticity at the 295°K isentropic level was $5 \times 10^{-5} \text{ s}^{-1}$. The SLP map and the cyclone trajectory are shown in Fig. 3. The detailed analysis was done for 11 January 2003 06 UTC, when the cyclone attained its maximum intensity. The 850-hPa geopotential height and temperature fields (Fig. 4) demonstrate the frontal structure of the cyclone. The 850-hPa thermal field indicates that the fronts (denoted in Fig. 4) are located slightly east of the cyclone center, implying that the cyclone has just reached its occlusion phase. The cloud structure,

seen in the high-resolution satellite image (which was available only for 11:55 UTC; Fig. 5), reflects the warm and the cold conveyor belts (to be described below) and the northern part of the cold front, along ~17°E.

The WCB (Fig. 6, thick arrow) was best identified on the 303°K isentropic surface. It was ~2,000 km long, extending from southern Libya (23° N, 19° E), southeast of the cyclone center, toward the Aegean Sea (40° N, 24° E) and climbing from 1.5 to 4.5 km. Similar ascent was noted by air-trajectory analysis. A band of cirrus clouds, of ~500 km width, coinciding with the WCB is clearly seen in the satellite image (Fig. 5). The clouds are thin in their southern

Fig. 4 The 850-hPa geopotential height and the temperature fields for January 11, 2003, 06 UTC together with the notation of the cold and warm fronts

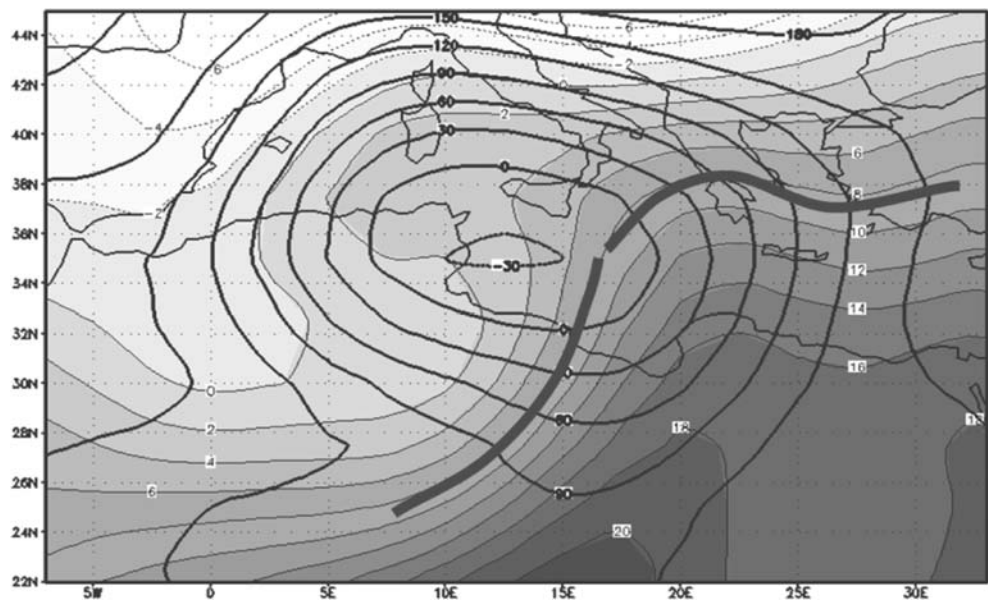
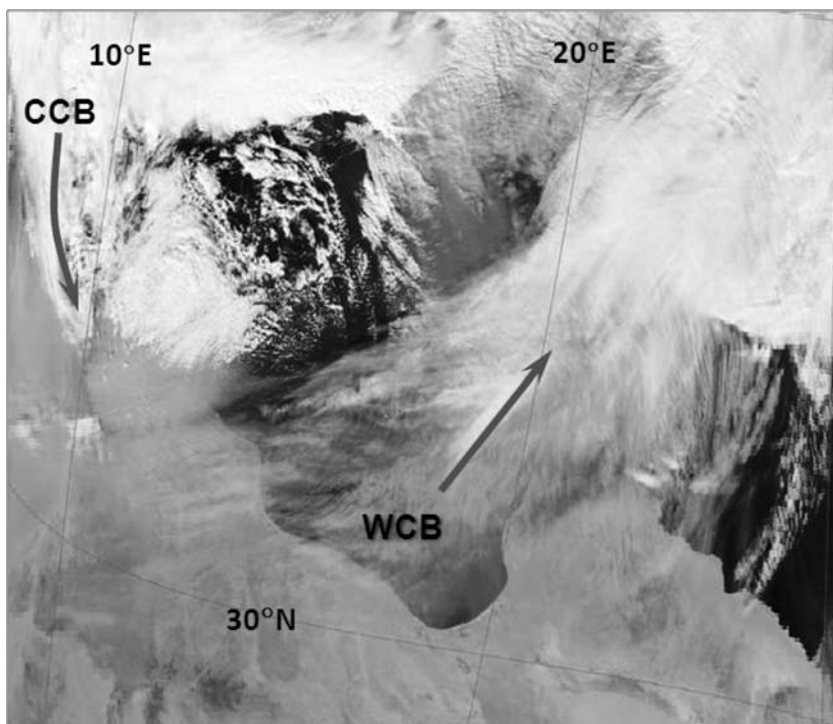


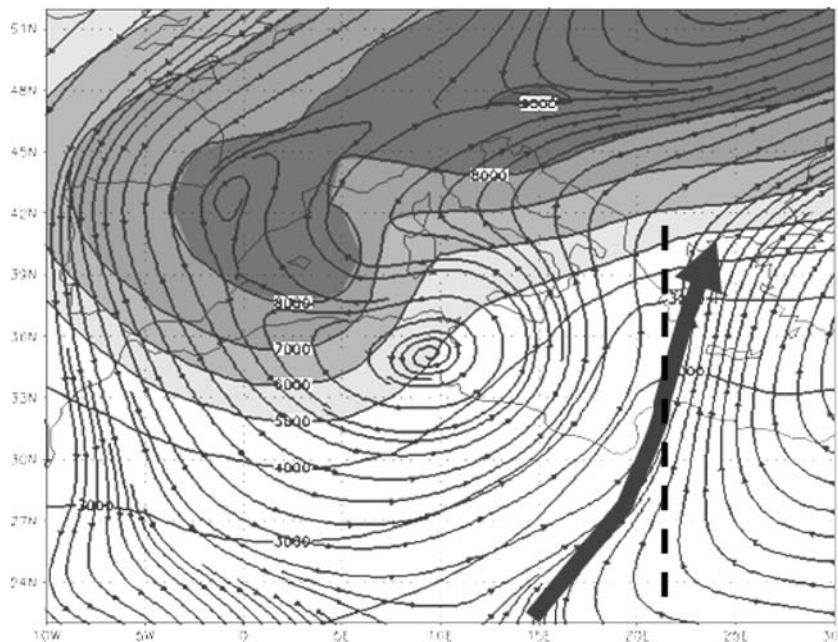
Fig. 5 MODIS satellite image of 2-km resolution for January 11, 2003, 11:55 UTC (http://www.nasa.gov/about/highlights/HP_Privacy.html#links)



part (near the North African coast) and become thicker northward where the air ascent within the conveyor belt is maximal. Figure 7 shows latitude-height cross-sections along 22° E longitude (coinciding with the WCB) of θ and θ_e (a) and RH (b). This Eulerian representation serves here as an estimate for the evolution of the RH within the warm air while moving along the WCB. The part of the

WCB south of 38° N is characterized by RH <30% (Fig. 7b), implying that this conveyor belt transports air which is originally dry. The increase in the RH along the WCB can be attributed to the sharp ascent, implied by the slope of the arrow representing it. The possibility of an upward moisture transport from the lower levels via convection is eliminated by the increase with height in

Fig. 6 Isentropic cross-section for the WCB on 303°K isentrope, January 11, 2003, 06 UTC. The *thick arrow* denotes the WCB and the *dashed line* denotes the location of the vertical cross-sections shown in Fig. 7



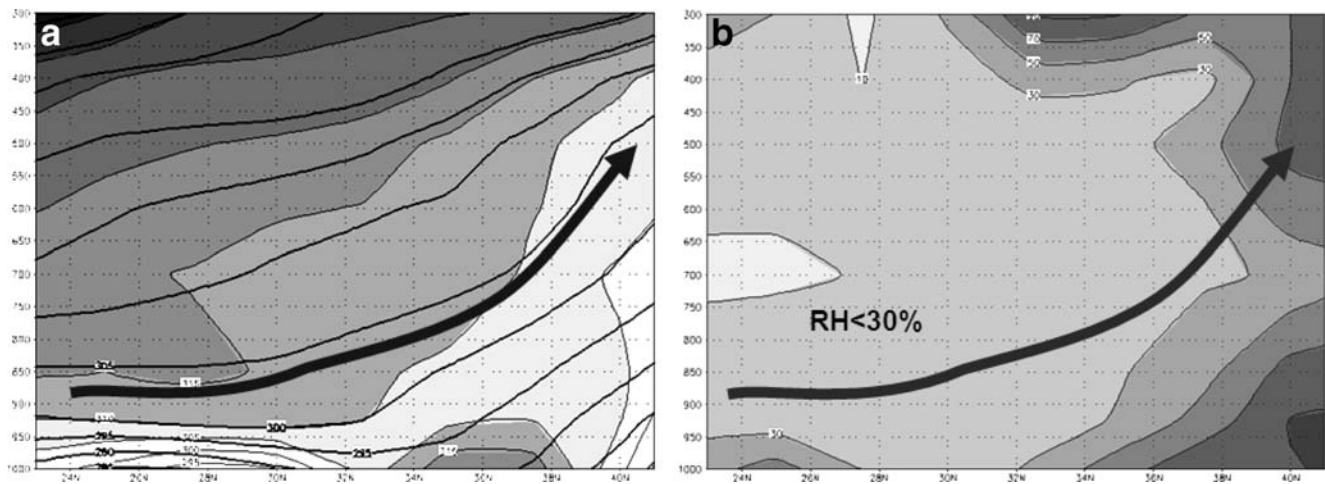


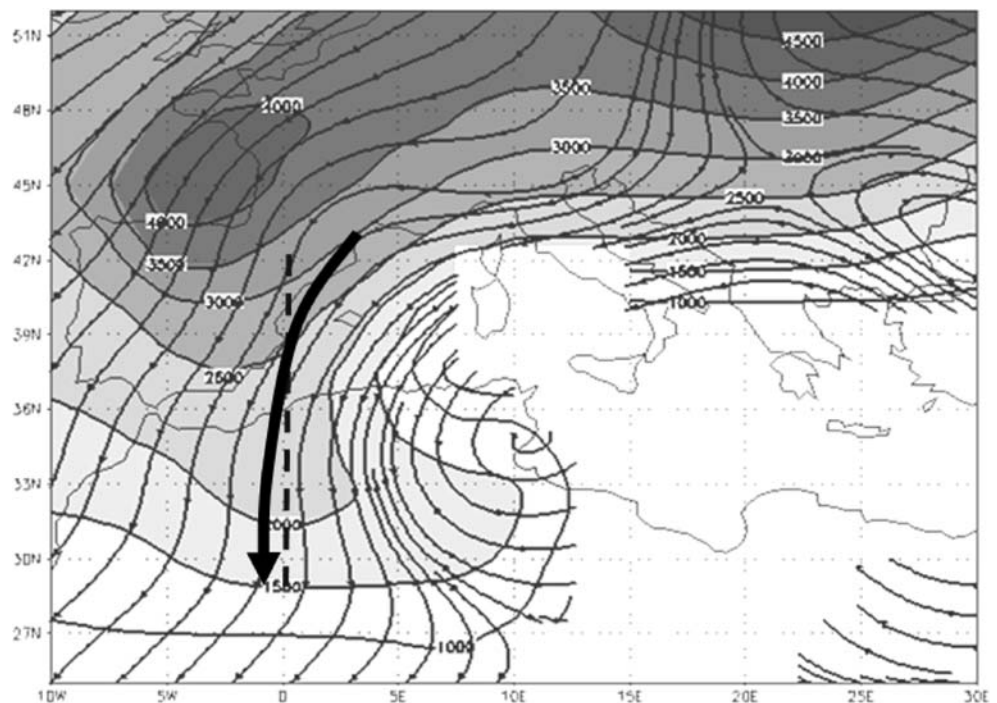
Fig. 7 Vertical-meridional cross-section of θ (thick lines) and θ_e (shaded) through the center of the WCB (a) and RH (b) along 22° E (the dashed line shown in Fig. 6). The thick arrows denote the WCB

both θ and θ_e beneath the WCB (Fig. 7a). This is also supported by the disconnection between the high RH within the WCB at its northern part and that found beneath it. The latter also indicates that the WCB cloudiness, including the northern denser part (Fig. 5) is composed mainly of cirrus clouds.

The CCB was most pronounced at the 288°K surface (Fig. 8). The cyclonic branch extends from the Gulf of Genoa, northwest of the cyclone center, encircling it from the west and ending at North Africa (around 29° N, 1° W), while descending from 3 to 1.5 km. No anticyclonic branch

was found. As for the WCB, vertical-meridional cross-sections of θ and θ_e and of RH (Fig. 9a, b, respectively) were done along 0° E (denoted by the dashed line in Fig. 8), which is parallel to the central and southern parts of the CCB. Since the air flow (as seen in air-trajectory analysis; not shown) was in the north–south direction, the cross-section approximates the evolution of the cold air mass while crossing the Mediterranean. The most pronounced change is an increase in moisture content. The RH increased from <20% to >80% along a 500-km distance (Fig. 9b) and θ_e increased considerably as well (Fig. 9a).

Fig. 8 Isentropic cross-section for the CCB on 288°K isentrope, January 11, 2003, 06 UTC. The thick arrow denotes the cyclonic branch of the CCB and the dashed line denotes the location of the vertical cross-sections shown in Fig. 9



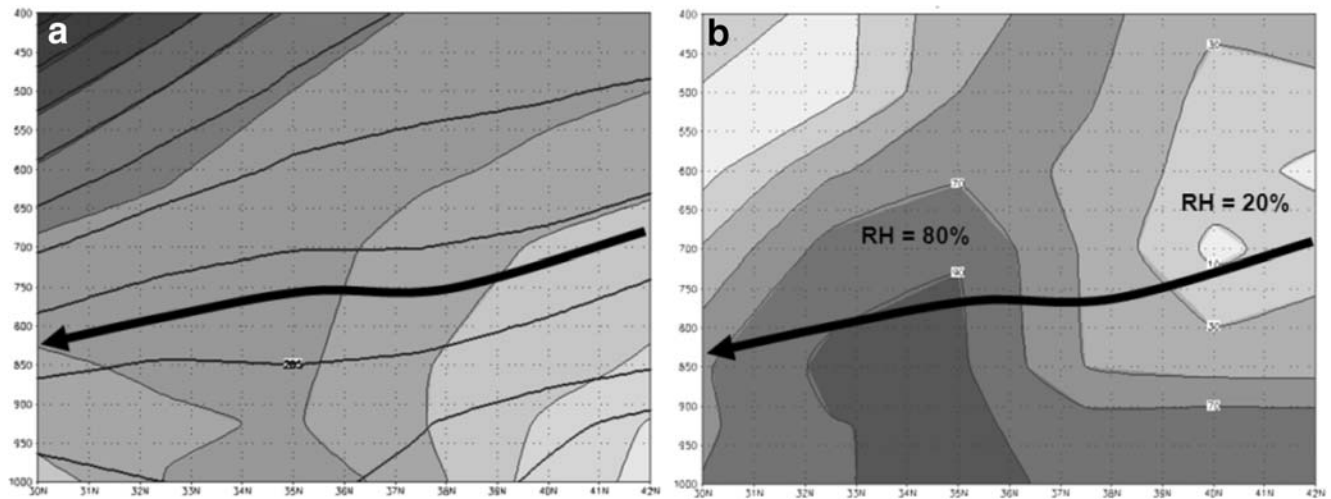


Fig. 9 As in Fig. 7, but for the CCB, along 0° E (the dashed line shown in Fig. 8)

The layer beneath the CCB north of 39° N is stratified, as implied by the increase in θ_e with height, but becomes mixed by convection to the south (downstream), as reflected by the almost uniform θ_e with height in the majority of the lower levels (Fig. 9a). South of 36° N, the convection becomes moist, as implied by the high RH ($>80\%$; Fig. 9b). These cross-sections suggest that the cold air, while moving over the Mediterranean, becomes moist and unstable, presumably by warming and moistening from below. A similar process was found by Shay-El and Alpert (1991) over the eastern Mediterranean within the cold air behind cold fronts of Cyprus Lows.

The DAI is seen in the 308°K PV as a long cyclonic band of high PV (Fig. 10a) and of low RH at the 400-hPa level (Fig. 10b). The 400-hPa is the closest pressure level to that of the isentrope in which the DAI was found. Both sections, together with the METEOSAT image of the water vapor channel (Fig. 10c), show a narrow strip extending from northwest sector of the cyclone that encircles it from southwest, ending ~ 100 km south of its center. No connection was found between the DAI and the reservoir of high PV to the north and the “hammerhead” shape (described by Browning 1990) was not found.

Figure 11 shows vertical-zonal cross-sections of θ and θ_e (a) and RH (b) along 37.5° N latitude. The cross-sections intersect the three conveyor belts and the northern part of the cyclone. The WCB (near 21° E, 700-hPa) is characterized by low RH, $<30\%$. The vertical increase in both θ and θ_e indicates that there is no convection there. The cyclonic branch of the CCB (near 1° E) is not homogeneous in its RH, which is high ($>90\%$), in its eastern part and drops sharply toward its western one. The absence of vertical change in θ_e at its eastern edge (and further eastward) indicates a thick layer of convection (also supported by the satellite imagery; Fig. 5). Near the cyclone center, the

vertical θ_e gradient and the medium RH ($<70\%$) indicate that convection does not take place there.

This case resembles the main features of the three conveyor belts described by the classical CBM, but differs from the classical CBM in several aspects. One is the absence of rain clouds within the WCB, second is the absence of anticyclonic branch in the CCB, and third is a disconnection between the DAI and the reservoir of high PV to the north of the cyclone.

The analysis done for the cyclone described above was repeated for the other seven cyclones. The results are summarized in Table 2. The WCBs had an average meridional extent of 1,700 km, about half that described by Browning (1990) for Atlantic cyclones and their vertical ascent was 3.3 km, in agreement with Browning (1990). The anticyclonic branch of the CCB was found only in half of the studied cyclones, and even when found, did not merge with the WCB, as described in the CBM (Browning 1990). DAIs were found in all of the cyclones, but they had maximum which was disconnected from the high-PV reservoir or connected to it by a thin streamer. In three cases, the maximum was collocated with the cyclone center (entitled “cutoff” in Table 2) and in the others—as a cyclonic curved band to the west of the cyclone. In addition, the DAIs lacked the “hammerhead” shape and their accompanying diffluent streamlines described in the CBM. The existence of WCB, cyclonic branch of the CCB, and DAI in each of the studied cyclones reflects the affinity of the MCs to the common midlatitude cyclones.

3.2 Moisture supply

The main contributor of cloudiness and precipitation in the “classical” midlatitude cyclones is the WCB (Browning

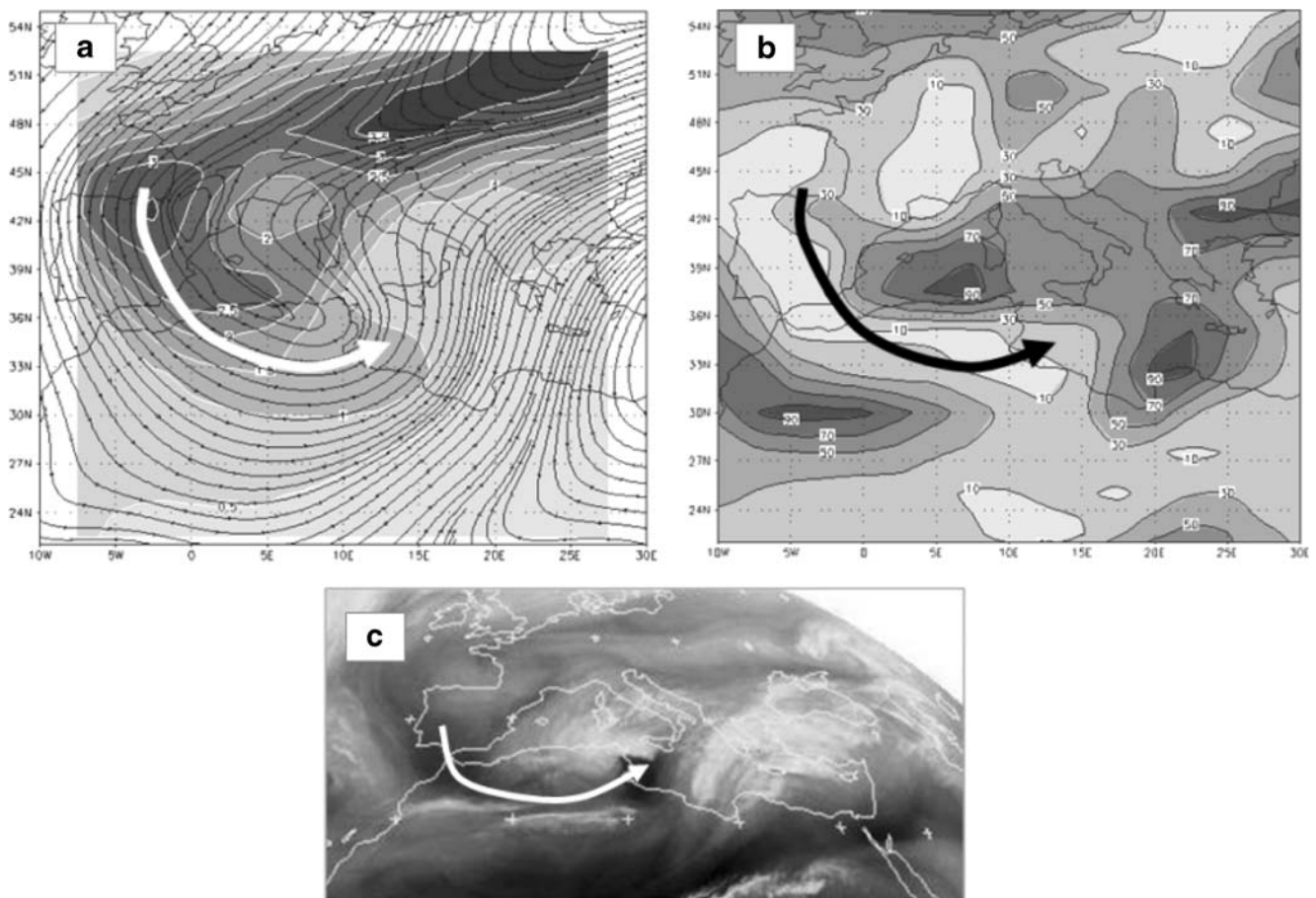


Fig. 10 The DAI as seen in the 308K isentropic potential vorticity (in potential vorticity units, **a**), in the 400-hPa RH (**b**), and in the METEOSAT water vapor channel (**c**) for January 11, 2003, 06 UTC. The *thick arrow* in each of them denotes the DAI

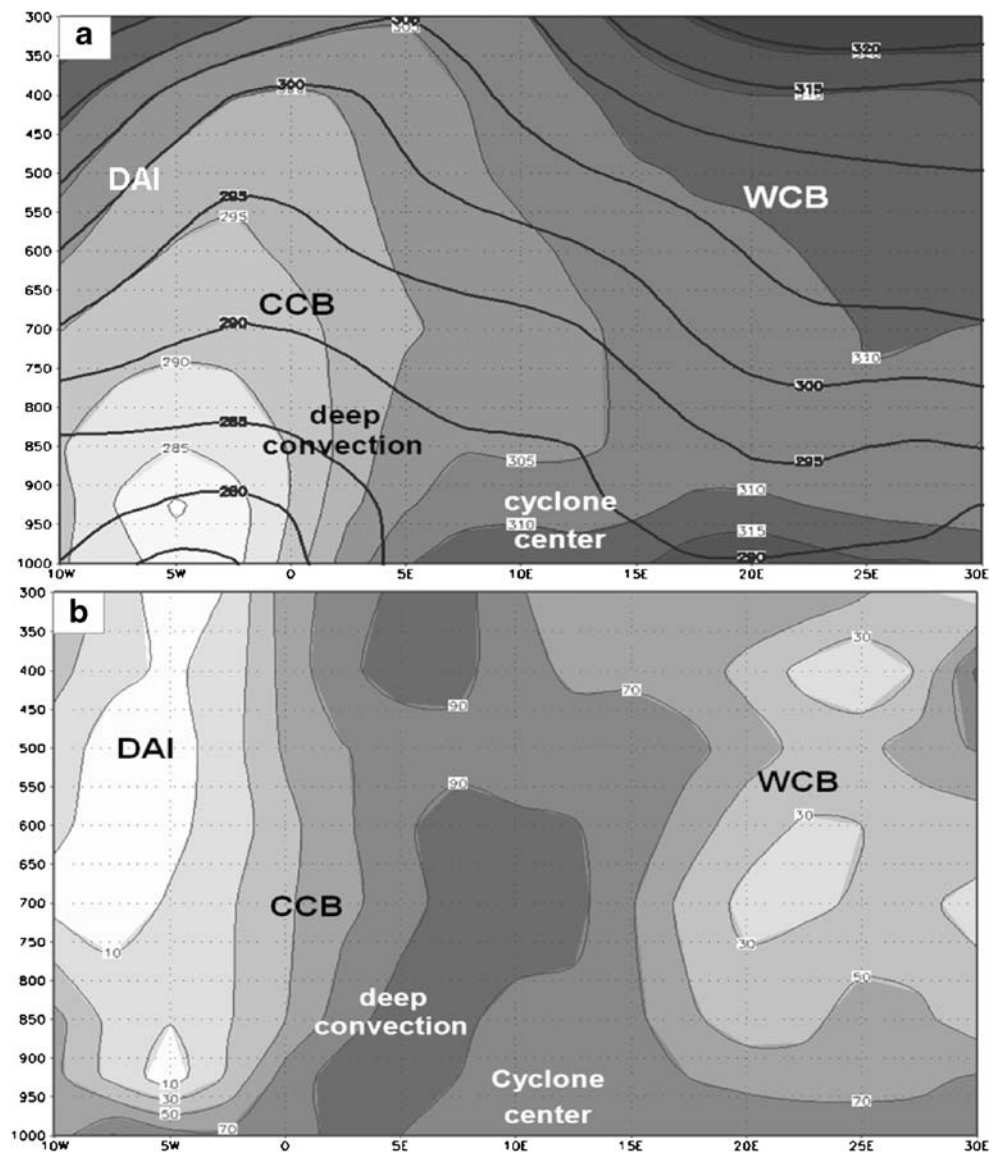
1990; Eckhardt et al. 2004), which is characterized by its massive cloud band. However, in five of the MCs studied here, the WCB had unorganized cloudiness, which was mostly confined to its northern part or being medium–high level (Table 2). The relatively poor cloudiness associated with the WCBs suggests that the moisture content of the warm air was low, presumably due to its being originated from the arid regions of North Africa. The origin of the warm air entering the WCBs was analyzed through Lagrangian backward trajectories. For each WCB, three trajectories, separated from each other by 100 km in the east–west direction, of 36-h paths were derived, starting from the latitude of the cyclone center. The use of three trajectories was done in order to validate that they were coherent before entering the WCB. In five of the cyclones, the origin of the warm air is the North African deserts, and even in the other two cases, in which the origin is in the Atlantic, the air has an arid path of >12 h.

An examination of the RH within the WCBs for the eight cyclones was done using vertical-zonal cross-sections along the latitude of the cyclones' centers

(Fig. 12). The values varied between 60% and 90%, except for the case of 10–12 January 2003, when it was only 30%. Inspection of the vertical ascent of the warm air masses within the WCBs indicates that, while reaching the latitude of the cyclone center (shown in the cross-sections; Fig. 12), they had already experienced considerable ascent of several kilometers. This explains the high RH found in most of the WCBs. The existence of cloudiness only in the northern part of the WCB in five of the studied cyclones suggests that the necessary condition for warm air to develop cloudiness is the considerable ascent or vertical moisture flux from the Mediterranean surface (as implied by the location of the cyclones' centers in the north of the Mediterranean).

In order to demonstrate which of the two conditions, the air ascent or the vertical moisture flux, is more important, we derived two vertical-zonal cross-sections of RH for the cyclone of 10–12 January 2003 (see Section 3.1): one along the northern coasts of the Mediterranean (42.5° N; Fig. 13a) and another along the North African coast (32.5° N; Fig. 13b), i.e., from both

Fig. 11 Vertical-zonal cross-sections through the cyclone, along 37.5° N: **a** θ (thick lines) and θ_e (shaded) and **b** RH. The WCB (pointing toward the page), the DAI, and the CCB (both pointing toward the reader) are denoted



sides of the cross-section shown in Fig. 11b. The WCB was found dry at the southern coast (RH <30%; Fig. 13b) and wet at the northern coast (RH >90%; Fig. 13a). The vertical increase in θ_e in the lower levels beneath the WCB (Fig. 11a), reflecting stable conditions, and the minimum in the RH there (Fig. 13b) eliminate the possibility that vertical moisture flux from the sea surface contributes moisture to the WCB. Therefore, the considerable ascent is the explanation for the high RH within the WCB. This was further examined, for the eight studied cyclones, by tracking the change in the RH of individual air parcels within the WCBs as a function of their elevation and location. In six of the eight cases, the RH of the air parcels increased just while they accelerated upward rather than while moving over the Mediterranean.

As for the CCB, Fig. 13 shows that it is extremely dry at the northern coasts of the Mediterranean (<20%; Fig. 13a)

and highly moist at the southern coast (>80%; Fig. 13b). Since air ascent is not observed along this belt, the increase in RH may be explained only by moisture fluxes from the Mediterranean Sea. The absence of vertical gradient in θ_e beneath the CCB (see Figs. 9a and 11a) suggests that convection exists there and, therefore, supports this hypothesis. Similar analysis derived for the other studied cyclones showed the same features for both the WCBs and the CCBs.

Air-trajectory analysis was done for the CCBs. The backward trajectories (not shown) indicated that, in part of the cyclones, the cold air originated from Europe, north of the Alps, and the Balkan, and in others, it originated from the northern part of the Mediterranean itself. Forward trajectories indicate that, in all cases, the southward end of the CCBs reached 30° N and southwards, i.e., the North African coast.

Table 2 Conveyor belts characteristics of the studied cyclones

Type of conveyor belt	WCB			CCB—cyclonic branch		CCB— anticyclonic branch	DAI structure
	Dates of existence	Meridional extent (km)	Cloudiness	Origin of air and ascent (km)	Descent (km)	Cloudiness	
16–18 Jan 2002	1,300	Partial, in the northern part	Atlantic, through Sahara 4.5	1.0	Shallow, beneath the CCB	–1.0	Cutoff
10–13 Mar 2002	1,600	Continuous band, medium–high	Sahara 2.5	0.8	Developed, convective left of the CCB	Not found	Cutoff and thin streamer
22–23 Mar 2002	1,800	At the northern part—convective	Mediterranean 3	2.0	No	2	Pronounced band
6–8 Jan 2003	2,000	At its western edge, along the cold front	Sahara 3	2.5	Low and shallow	Not found	Cutoff and thin streamer
10–12 Jan 2003	2,000	Thick only in the northern part	Sahara 3	1.5	Deep, convective	Not found	Pronounced band
17–20 Jan 2003	1,600	Thick	Sahara 2	0	Scattered, mainly to the left	–0.5	Cutoff
26–28 Jan 2003	1,650	At the northern part	Sahara 3.5	0.5	Convective	0	Distinct maximum and streamer
31 Jan–2 Feb 2003	1,300	At the northern part: unorganized	Atlantic, through Sahara 5	2.0	Convective	Not found	Cutoff
Average and SD	1,700±270		3.3±1.0	1.3±0.9		Inconsistent	

The term “cutoff” for DAI refers to the case in which positive PV anomaly coincides with the cyclone center

4 Summary and discussion

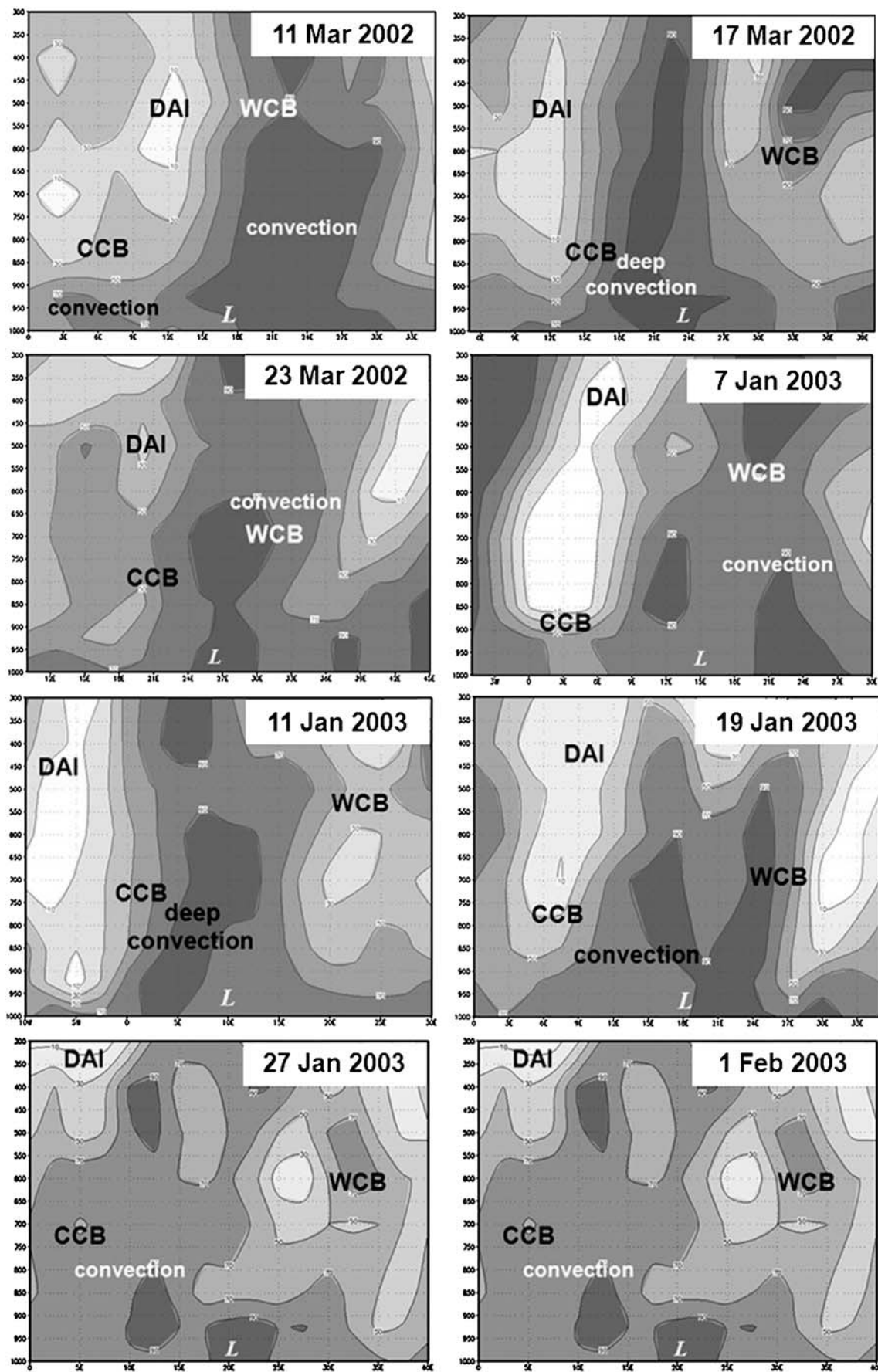
The existence, structure, and cloudiness of the conveyor belts are examined here for eight winter MCs. These cyclones are expected to resemble the main features of the midlatitude cyclones with several deviations due to the following geographical and climatological factors:

1. The Mediterranean, extending between 30° and 42° N, is situated south of the global climatic midlatitude cyclones belt and, therefore, is closer to the descending branch of the Hadley cell with its suppressive effect on cyclogenesis and vertical ascent.
2. The warm air mass involved in the MCs originates from the arid Saharan Desert, so that the WCB is not the main precipitation contributor or a source of moisture for the CCB (via raindrops fall into the CCB).
3. While considering the role of conveyor belts in rain production, the convection cannot be ignored, since the relatively warm water of the Mediterranean Sea act in the winter as a source of latent and sensible heat and moisture, shown by Shay-El and Alpert (1991) and Stein and Alpert (1993) for the eastern Mediterranean.

The analysis of the eight MCs indicates the existence of the main features of the CBM. The three conveyor belts were identified clearly in the isentropic maps, except for the

anticyclonic branch of the CCB, which was absent in half of the studied cyclones, and the DAI, which was not fully connected to the high-PV reservoir north of the cyclone in seven of the cases. This is consistent with the existence of upper-level cutoff lows in association with half of the study cyclones and indicates that the MCs develop when the positive PV anomaly has almost disconnected from the PV reservoir to the north. However, the existence of DAI in all of the studied MCs suggests that they indeed belong to the family of midlatitude cyclones, from the perspective of stratospheric PV involvement. The cloud patterns associated with the WCB and the cyclonic branch of the CCB appeared in the majority of these cyclones, but no signature of CCB’s anticyclonic branch was found in the satellite imagery.

The cloudiness associated with the WCB was mostly high and medium and, therefore, seem not to be the main precipitation contributors for MCs, despite the considerable ascent observed within these belts. This is in contrast with the findings of Eckhardt et al. (2004) that “WCB trajectory produces, on average, about six times as much precipitation as an extratropical trajectory starting from 500 m.” The nature of the cloudiness associated with the WCB in the MCs is explained by the arid origin (Saharan Desert) of the warm air in most of them, which is supported by back-trajectory analysis. Vertical cross-sections along the WCBs indicate that the dominant factor for the cloud formation was the air



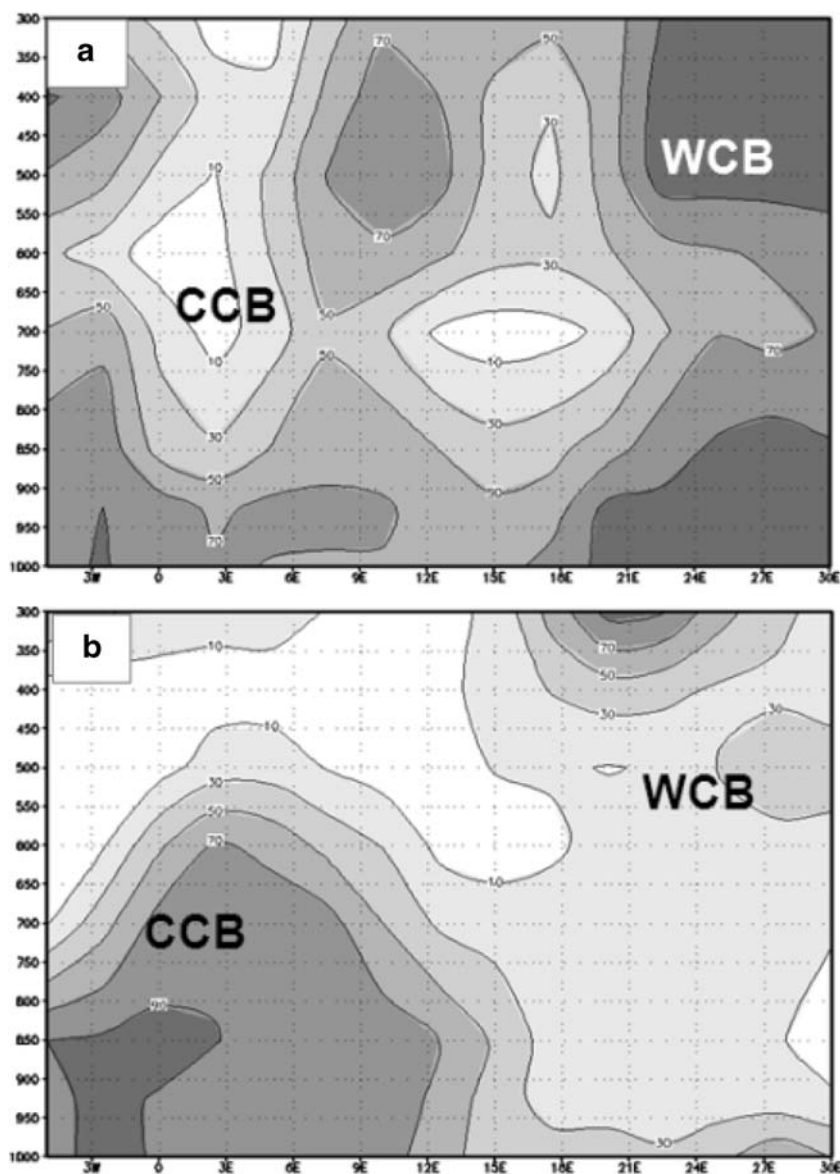
◀ **Fig. 12** Vertical-zonal cross-sections of RH through the cyclones' centers. The WCB (pointing toward the page), the DAI, and the CCB (both pointing toward the reader) are denoted

ascent, of several kilometers, rather than vertical moisture transport from the Mediterranean surface. A possible explanation for that is the stability expected to exist below the warm air mass and the large separation between the WCB and the sea surface, being >2,000 m.

The cloud bands associated with the cyclonic branch of the CCBs were found in all the studied cyclones, and in some of them, were even more pronounced than those associated with the WCB. Vertical cross-sections indicate the important role of vertical moisture fluxes from the warm Mediterranean surface via convection, as was also found by Shay-El and Alpert (1991) and Stein and Alpert (1993).

To conclude, the winter MCs resembles the majority of the features characterizing midlatitude cyclones. The differences between them and the classical ones can be attributed to the geographic-climatic unique features of this region and their being south of the winter midlatitude Atlantic storm tracks. Also, considerable differences were found between the individual cyclones in the moisture content of the WCBs (and their related cloudiness), in the convection within the cold air mass, and in the existence of the anticyclonic branch in the CCBs. This can be explained by the regional complexity and the limited moisture sources. The sample of eight MCs studied here indicates that the main condition for rain is not necessarily the existence of conveyor belts, but the onshore flow of cold air that move over the warmer Mediterranean Sea surface. The differences among the individual cyclones suggest that, in order

Fig. 13 Vertical-zonal cross-sections of RH along 42.5° N (a) and 32.5° N (b), January 11, 2003, 06 UTC



to obtain reliable climatology for the MCs, a more extensive study has to be performed.

Acknowledgement This study was supported by the Israeli Science Foundation (ISF, grants 764/06 and 1084/06) and by the European Union Marie Curie International reintegration grant MIRG-CT-2005-016835. The NCEP/NCAR reanalysis have been obtained from the National Oceanic and Atmospheric Administration (NOAA).

References

- Alpert P, Ganor E (1994) A jet stream associated heavy dust storm in the western Mediterranean. *J Geophys Res* 98(D4):7339–7349
- Alpert P, Neeman BU (1992) Cold small-scale cyclones over the eastern Mediterranean. *Tellus* 44A:173–179
- Alpert P, Ziv B (1989) The Sharav cyclone: observation and some theoretical considerations. *J Geophys Res* 94:18495–18514
- Alpert P, Neeman BU, Shay-El Y (1990) Climatological analysis of Mediterranean cyclones using ECMWF data. *Tellus* 42A:65–77
- Alpert P, Tzidulko M, Izigsohn D (1999) A shallow short-lived meso-beta cyclone over the gulf of Antalya, eastern Mediterranean. *Tellus* 51A:249–262
- Bader MJ, Forbes GS, Grant JR, Lilley RBE, Waters AJ (1995) Images in weather forecasting. A practical guide for interpreting satellite and radar imagery. Cambridge University Press, Cambridge, p 499
- Bolton D (1980) The computation of equivalent potential temperature. *Mon Weather Rev* 108:1046–1053
- Browning KA (1990) Organization of clouds and precipitation in extratropical cyclones. In: Newton CW, Holopainen EO (eds) *Extratropical Cyclones. The Erik Palmén Memorial Volume*. American Meteorological Society, Boston, MA, pp 129–153
- Browning KA (1997) The dry intrusion perspective of extra-tropical cyclone development. *Meteorol Appl* 4:317–324
- Browning KA (1999) Mesoscale aspects of extratropical cyclones: an observational perspective. In: Shapiro MA, Grønås S (eds) *The life cycles of extratropical cyclones*. American Meteorological Society, Boston, MA, pp 265–283
- Browning KA, Golding BW (1995) Mesoscale aspects of a dry intrusion within a vigorous cyclone. *Q J R Meteorol Soc* 121:463–493
- Browning KA, Roberts NM (1996) Variation of frontal and precipitation structure along a cold front. *Q J R Meteorol Soc* 122:1845–1872
- Campins J, Genovés A, Jansà A, Guijarro A, Ramis C (2000) A catalogue and a classification of surface cyclones for the Western Mediterranean. *Int J Climatol* 20(9):969–984
- Carlson TN (1980) Airflow through mid-latitude cyclones and the comma cloud pattern. *Mon Weather Rev* 108:1498–1509
- Carlson TN (1987) Cloud configuration in relation to relative isentropic motion. In: Bader M, Waters T (eds) *Preprints, U.K. Met. Office Workshop on Satellite and Radar Imagery Interpretation, EUMETSAT*, pp 43–61
- Carlson TN (1991) *Mid-latitude weather systems*. Harper Collins, London, p 507
- Carr FH, Millard JP (1985) A composite study of comma clouds and their association with severe weather over the Great Plains. *Mon Weather Rev* 113:370–387
- Cohen RA (1993) An air stream analysis of the occluded cyclone. Ph.D. dissertation, Drexel University, 209 pp (Available from Department of Physics and Atmospheric Science, Drexel University, 3141 Chestnut Street, Philadelphia, PA 19104-2875)
- Durran DR, Weber DB (1988) An investigation of the poleward edges of cirrus clouds associated with mid-latitude jet streams. *Mon Weather Rev* 116:702–714
- Eckhardt S, Stohl A, Wernli H, James P, Forster C, Spichtinger N (2004) A 15-year climatology of warm conveyor belts. *J Clim* 17(17):218–237
- Gall R, Shapiro M (2000) The influence of Carl-Gustaf Rossby on mesoscale weather prediction and an outlook for the future. *Bull Am Meteorol Soc* 81:1507–1523
- Gurka JJ, Auciello EP, Gigi AF, Waldstreicher JS, Keeter KK, Businger S, Lee LG (1995) Winter weather forecasting throughout the eastern United States. Part II: an operational perspective of cyclogenesis. *Weather Forecast* 10:21–41
- Her Majesty, Meteorological Office (HMSO) (1962) *Weather in the Mediterranean*, 1, London, 362 pp
- Hoskins BJ, Hodges KI (2002) New perspectives on the Northern Hemisphere winter storm tracks. *J Atmos Sci* 59:1041–1061
- HYSPLIT4 (Hybrid Single-Particle Lagrangian Integrated Trajectory) Model (1997) NOAA Air Resources Laboratory, Silver Spring, MD. Available at <http://www.arl.noaa.gov/ready/hysplit4.html>
- Kahana R, Ziv B, Enzel Y, Dayan U (2002) Synoptic climatology of major floods in the Negev Desert, Israel. *Int J Climatol* 22:867–822
- Kain JS, Goss SM, Baldwin ME (2000) The melting effect as a factor in precipitation-type forecasting. *Weather Forecast* 15:700–714
- Kalnay E, Kanamitsu M, Kistler R, Collins W, Deaven D, Gandin L, Iredell M, Saha S, White G, Woollen J, Zhu Y, Chelliah M, Ebisuzaki W, Higgins W, Janowiak J, Mo KC, Ropelewski C, Wang J, Leetmaa A, Reynolds R, Jenne R, Joseph D (1996) The NCEP/NCAR 40-year reanalysis project. *Bull Am Meteorol Soc* 77:437–471
- Kistler R, Kalnay E, Collins W, Saha S, White G, Woollen J, Chelliah M, Ebisuzaki W, Kanamitsu M, Kousky V, Van Den Dool H, Jenne R, Fiorino M (2001) The NCEP–NCAR 50-year reanalysis: monthly means CD-ROM and documentation. *Bull Am Meteorol Soc* 82:247–267
- Kurz M (1988) Development of cloud distribution and relative motions during the mature and occlusion stage of a typical cyclone development. Preprints, Palmén Memorial Symposium on Extratropical Cyclones, Helsinki, Finland, American Meteorological Society, pp 201–204
- Kutzbach G (1979) *The thermal theory of cyclones*. American Meteorological Society, Boston, MA, p 255
- Martin JE (1999) Quasigeostrophic forcing of ascent in the occluded sector of cyclones and the trowal airstream. *Mon Weather Rev* 127:70–88
- Radinovic D (1987) *Mediterranean cyclones and their influence on the weather and climate*. WMO, PSMP Rep. Ser. No. 24
- Reiter ER (1975) *Handbook for forecasters in the Mediterranean*. Naval Postgraduate School, Monterey, California
- Romem M, Ziv B, Saaroni H (2007) Scenarios in the development of Mediterranean cyclones. *ADGEO* 12:59–65
- Schultz DM (2001) Reexamining the cold conveyor belt. *Mon Weather Rev* 129:2205–2225
- Shaw WN (1903) The meteorological aspects of the storm of February 26–27, 1903. *Q J R Meteorol Soc* 29:233–258
- Shay-El Y, Alpert P (1991) A diagnostic study of winter diabatic heating in the Mediterranean in relation to cyclones. *Q J R Meteorol Soc* 117:715–747
- Stein U, Alpert P (1993) Factor separation in numerical simulations. *J Atmos Sci* 50:2107–2115
- Tafferner A, Egger J (1990) Test of theories of lee cyclogenesis: ALPEX cases. *J Atmos Sci* 47(20):2417–2428

- Trigo IG, Bigg GR, Davies TD (2002) Climatology of cyclogenesis in the Mediterranean. *Mon Weather Rev* 130:549–569
- Tsidulko M, Alpert P (2001) Synergism of upper-level potential vorticity and mountains in Genoa lee cyclogenesis—a numerical study. *Meteor Atmos Physics* 78(3/4):261–285
- Wernli H (1995) Lagrangian perspective of extratropical cyclogenesis. Dissertation no. 11016, Swiss Federal Institute of Technology (ETH), Zürich, 157 pp
- Wernli H (1997) A Lagrangian-based analysis of extratropical cyclones. II: a detailed case-study. *Q J R Meteorol Soc* 123:1677–1706
- Wernli H, Davies HC (1997) A Lagrangian-based analysis of extratropical cyclones. I: the method and some applications. *Q J R Meteorol Soc* 123:467–489
- Young MV, Monk GA, Browning KA (1987) Interpretation of satellite imagery of a rapidly deepening cyclone. *Q J R Meteorol Soc* 113:1089–1115